

NONLINEAR-OPTICAL PHENOMENA DOI: 10.1070/QEL16120

Nonlinear processes upon two-photon interband picosecond excitation of $PbWO_4$ crystal

V.I. Lukanin, A.Ya. Karasik

Abstract. **A new experimental method is proposed to study the dynamics of nonlinear processes occurring upon two-photon interband picosecond excitation of a lead tungstate crystal and upon its excitation by cw probe radiation in a temporal range from several nanoseconds to several seconds. The method is applied to the case of crystal excitation by a sequence of 25 high-power picosecond pulses with a wavelength of 523.5 nm and 633-nm cw probe radiation. Measuring the probe beam transmittance during crystal excitation, one can investigate the influence of two-photon interband absorption and the thermal nonlinearity of the refractive index on the dynamics of nonlinear processes in a wide range of times (from several nanoseconds to several seconds). The time resolution of the measuring system makes it possible to distinguish fast and slow nonlinear processes of electronic or thermal nature, including the generation of a thermal lens and thermal diffusion. An alternative method is proposed to study the dynamics of induced absorption transformation and, therefore, the dynamics of the development of nonlinear rocesses upon degenerate two-photon excitation of the crystal in the absence of external probe radiation.**

Keywords: *two-photon excitation, thermal lens, nonlinear effects, thermal diffusion.*

1. Introduction

Interband two-photon absorption (TPA) in materials opens new possibilities in the case of excitation of electron states in the conduction band, where the materials are almost opaque, while one-photon absorption (OPA) at the same excitation energies makes it possible to perform an analysis using mainly luminescence spectroscopy methods. In contrast to OPA, in the case of interband TPA, when the energy of each photon correspond to the transparency window of the medium, one can implement in practice uniform volume excitation of the crystal by the total energy of two photons and eliminate the nonradiative loss in the surface layer of the material, which depend on the quality of its surface and radically affect the correctness of measurements of the quantum yield and luminescence spectra. Along with the well-developed methods of linear absorption and luminescence spectroscopy, the use of two-photon nonlinear spectroscopy opens additional possibilities, related to selective excitation of electron states in the conduction band and study of the luminescence from these states.

The generation of radiation in nonlinear media due to two-photon transitions was considered for the first time by Prokhorov [1, 2] and Selivanenko. Letokhov [3] proposed to use two-photon amplifiers to form ultrashort light pulses. Different optical schemes were theoretically investigated and different nonlinear media (mainly organic compounds and gases (see [3–5] and references therein)) were proposed for two-photon amplification. A possibility of designing a two-photon pulsed atomic lithium vapour laser was shown in [6]. A cw two-photon atomic barium vapour laser was reported in [7], and a two-photon potassium vapour laser was demonstrated in [8].

The nonlinear processes of two-photon absorption have been actively studied during the last decade, as is evidenced by more than a hundred recent publications on this subject [9]. However, there are practically no new experimental studies on the two-photon amplification. In our opinion, the reason is the competition of two-photon amplification with a number of related nonlinear electronic and thermal processes, which manifest themselves upon excitation of a nonlinear medium by laser beams with different intensities and pulse durations, beginning with femtosecond pulses and up to cw radiation [10, 11]. In this paper we show how our attempts to reveal the interband two-photon amplification in a $PbWO_4$ crystal failed because of the competition of amplification with other nonlinear effects of different natures.

The experimental method proposed by us, which is based on the use of high-power picosecond excitation of the crystal and cw probe radiation, makes it possible to investigate (with a high time resolution) nonlinear processes with relaxation times exceeding by many orders of magnitude the ranges of electronic nonlinearity relaxation times; the relaxation times determined by the free-carrier transport in the conduction band; and the relaxation times related to the thermal nonlinearity, which leads to the formation of a thermal lens. This approach allows one to delimit the regions of influence and development rates of different nonlinearities in a wide range of times. It is based, in particular, on the dynamics of generation of induced absorption and accumulation of electronic excitations in crystals pumped by picosecond laser pulses, which was investigated by us in [12–14]. As a result, as will be shown below, having measured the crystal transmittance at the probe light wavelength, one can estimate the excitation intensity leading to the TPA and thermal effect, as well as the thermal diffusion times, which determine the formation and decay rates of thermal lens.

V.I. Lukanin, A.Ya. Karasik A.M. Prokhorov General Physics Institute, Russian Academy of Sciences, ul. Vavilova 38, 119991 Moscow, Russia; e-mail: karasik@lst.gpi.ru

Received 28 April 2016; revision received 8 July 2016
Kvantovaya Elektronika **46** (9) 806–810 (2016)
Translated by Yu.P. Sin'kov

2. Schematic of the experiment

The experimental study was performed on a 28-mm-long $PbWO_4$ crystal, cut in the form of a parallelepiped; previously we investigated two-photon absorption in this crystal [12–15]. The laser excitation of the crystal was performed by linearly polarised light. According to different data, the crystal band gap varies within 3–4.7 eV (see [15] and references therein). The TPA coefficients in $PbWO_4$ excited by a laser beam with a wavelength of 523.5 nm, depending on the linear polarisation direction, vary from 1.2 to 0.6 cm GW^{-1} [13, 15].

Two-photon excitation of the sample was performed by the second-harmonic radiation ($2h\nu_{exc}$ = 4.73 eV) of an $YLiF:Nd^{3+}$ laser. A schematic of the experimental setup is presented in Fig. 1.

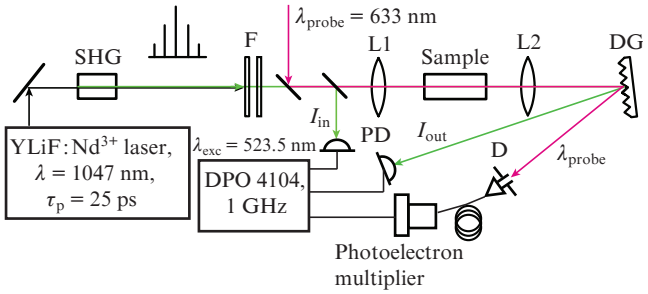

Figure 1. Schematic of the experimental setup.

The passive mode-locked *Q*-switched laser emitted trains of picosecond pulses with a total duration of ~150 ns (τ_p = 25 ps). After the frequency doubling in the second-harmonic crystal (SHG–$LiIO_3$), the laser beam intensity (λ_{exc} = 523.5 nm) was attenuated to the necessary level by neutral filters F, and the fundamental wavelength (λ = 1047 nm) was cut off. The amplitudes of train pulses before and after the crystal (I_{in} and I_{out}) were measured using fast silicon pin photodiodes PD and analysed on a DPO 4104 digital oscilloscope with a transmission band of 1 GHz.

Collinearly directed Gaussian single-mode beams of picosecond laser excitation (λ_{exc} = 523.5 nm) and cw probe He–Ne laser radiation (λ = 633 nm) were focused by lens L1 (f = 112 or 250 mm) into the centre of the crystal under study (the maximum single-pulse intensity in the train reached ~100 GW cm^{-2}). Note that both picosecond pump radiation and probe red light fall in the transparency window of the crystal and do not suffer additional loss. The pump spot radius in the lens focus (f = 112 mm) was 16 μm (at the $1/e^2$ level), the beam waist length was 6 mm, and the probe light spot radius was 80 μm at a probe power of 8 μW (for the lens with f = 250 mm, the pump spot radius in the focus was 36 μm and the beam waist length was 30 mm). Enlarged images of pump and probe beam spots after lens L2 were formed on diffraction grating DG. Then the probe beam with a diameter of ~20 mm was directed to iris diaphragm D with a diameter of 4 mm, which could be gradually displaced perpendicularly to the beam axis. The light transmitted through the diaphragm was introduced (using a lens) into an optical fibre and arrived at a FEU-136 photoelectron multiplier. The picosecond excitation beam diffracted by the grating was directed to fast silicon pin photodiode PD with a photosensitive area 1 mm in diameter.

3. Experimental results

3.1. Dynamics of induced absorption at the probe light frequency

Figure 2 shows the kinetics of the probe light intensity, measured with the photoelectron multiplier during crystal excitation by high-power picosecond radiation. The diaphragm centre was aligned with the excitation and probe beam axes (in zero diffraction orders). It follows from the oscillograms in Fig. 2 that, after the crystal excitation, pulses with a duration of ~0.5 ms arise in the spectrum of cw He–Ne laser radiation. The pulse frequency was equal to the repetition rate of picosecond excitation trains, which was varied within 0.1–10 Hz. For focusing lens L1 with f = 112 mm, the 'positive' pulse amplitude in Fig. 2 was larger by a factor of 3–4 than for the case where the lens with a longer focal length (f = 250 mm) was used (i.e., at a lower excitation intensity and weaker crystal heating).

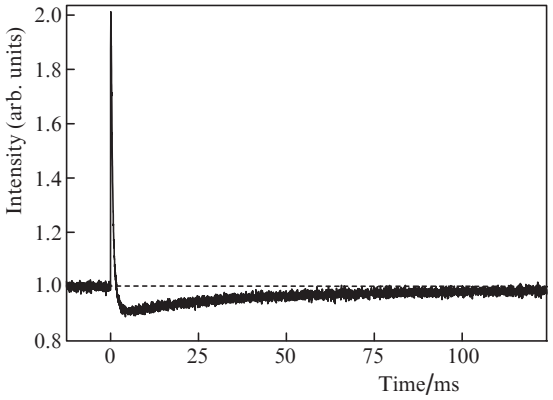

Figure 2. Oscillogram of the probe radiation during $PbWO_4$ crystal excitation by a train of pulses (λ_{exc} = 523.5 nm, $\boldsymbol{E}\|$C4, $\boldsymbol{k}\perp$C4) for the case where the diaphragm centre is aligned with the beam axes.

The oscillogram in Fig. 2 exhibits also a 'negative' spike with a relaxation time of several tens of milliseconds. The oscillogram recorded with the diaphragm displaced from the probe beam centre by a distance exceeding the diaphragm diameter (4 mm) contains only a negative spike (Figs 2, 3), which was explained by us in [14] as the result of single-photon absorption on the transitions from the electron levels excited due to two-photon absorption to the trap (defect) levels.

Note that the induced absorption is initiated even by the first, relatively weak excitation train pulses (Fig. 3). In the beginning of induced absorption pulse, one can observe a stage of rapid exponential rise with a rise constant of ~60 ns, which is followed by a stage of relatively slow rise with a characteristic time of ~10 μs [assigned by us to the migration of electronic excitation to crystal defects (traps)] and, finally, an excitation relaxation stage (Fig. 2) with a characteristic relaxation time of ~100 ms. A replacement of the probe light source having a wavelength λ = 633 nm with a 532-nm laser did not change much the oscillogram shape.

We verified if the positive pulse in the oscillogram presented in Fig. 2 indicates probe light amplification. Measurements of the probe light energy at the crystal input and output showed that the amplification is absent and that

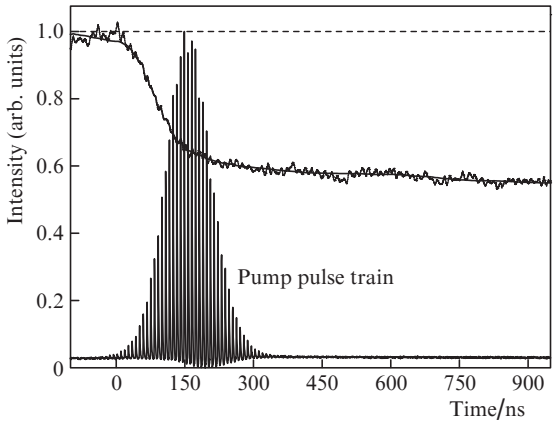

Figure 3. Oscillogram illustrating the kinetics of induced absorption during $PbWO_4$ crystal excitation (λ_{exc} = 523.5 nm, $\boldsymbol{E}\|$C4, $\boldsymbol{k}\perp$C4) by a train of pulses, when diaphragm D (Fig. 1) is displaced from the probe beam center by a distance exceeding its diameter.

the pulses arise in the cw radiation spectrum due to the generation of a thermal lens in the crystal and, as a consequence, beam focusing. The thermal lens was recorded using a CCD camera, located directly behind the output face of $PbWO_4$ crystal (at a distance of ~10 mm from end face) (Fig. 4).

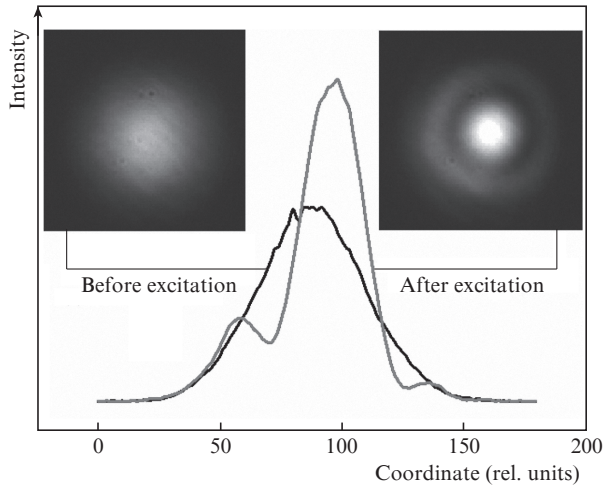

Figure 4. Formation of a thermal lens in a $PbWO_4$ crystal under picosecond pumping with λ_{exc} = 523.5 nm. The insets show the probe beam profiles before and after the crystal excitation.

One can see that the thermal lens is most pronounced in the paraxial region of crystal excitation by the pump beam, where the laser energy density is maximal. Note that the focal length of the induced lens depends, in particular, on the focal length of lens L1 (Fig. 1) and pump radiation parameters: pulse duration and power and thermooptical characteristics of the crystal.

Induced absorption is also observed in the excitation beam 'wings', i.e., at the periphery of the crystal cross section; it may be related to the spatial migration of the excitation energy through the crystal. A slight displacement of diaphragm D (Fig. 1) with respect to the probe beam centre first leads to a decrease in the probe radiation intensity due to the

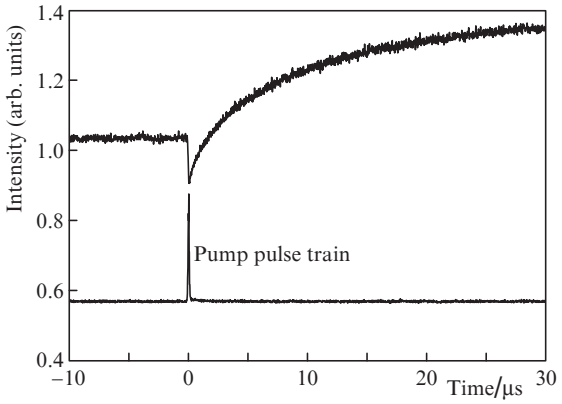

Figure 5. Oscillogram illustrating a fragment of the induced absorption kinetics and thermal lens formation at the probe light wavelength, with diaphragm D (Fig. 1) slightly displaced from the probe spot centre.

enhanced absorption from the excited state, but then the probe intensity increases as a result of the formation of thermal lens (Fig. 5).

3.2. Absorption transformation dynamics upon degenerate two-photon excitation

In the case of TPA, the excited crystal state absorbs also the third pump photon with a wavelength 523.5 nm, which can be considered as a probe photon. Thus, the transformation dynamics of the probe wave transmission can be investigated under conditions of degenerate two-photon excitation in the absence of external probe radiation. Here, we measured the time characteristics of radiation under picosecond excitation conditions using a fast silicon pin photodiode PD (Fig. 1). The PD photosensitive area was aligned with the centre of the picosecond excitation beam cross section, the diameter of which significantly exceeded the photodiode aperture.

Figures 6a and 6b present laser pulse oscillograms, recorded with the picosecond laser pump wavelength λ_{exc} = 523.5 nm at the input and output of the crystal at an excitation intensity of $I = 0.25I_{max}$ (I_{max} is the maximum peak intensity of the pulses in the train, which was used in the experiment). The intensity of the pulses at the train center, located symmetrically with respect to the instant t = 0 and having close amplitudes, decreases due to the TPA [12–15]. At $I = I_{max}$, the pattern radically changes (Fig. 6c). The intensity of the pulses in the left half of the train decreases and is limited due to the TPA, whereas the pulse intensity in the train trailing edge increases because of the thermal lens formation.

Figure 7 shows (i) the time dependence of the crystal transmittance I_{out}/I_{in}, obtained by dividing the amplitudes of the corresponding pulses in trains at the output (Fig. 6c) and input (Fig. 6a) of the crystal at the excitation intensity $I = I_{max}$ and (ii) the envelope of the excitation pulse train. The initial portion of the dependence (from −125 to −75 ns) demonstrates a successive decrease in the crystal transmittance for the first few train pulses as a result of the TPA dominance. Then the transmittance becomes minimal in the vicinity of --50 ns and starts rising with an increase in the pulse number in the train in the range of times from −50 to 125 ns. This dependence demonstrates the dynamics of crystal transmittance transformation for the probe beam under conditions of competition between several nonlinear processes.

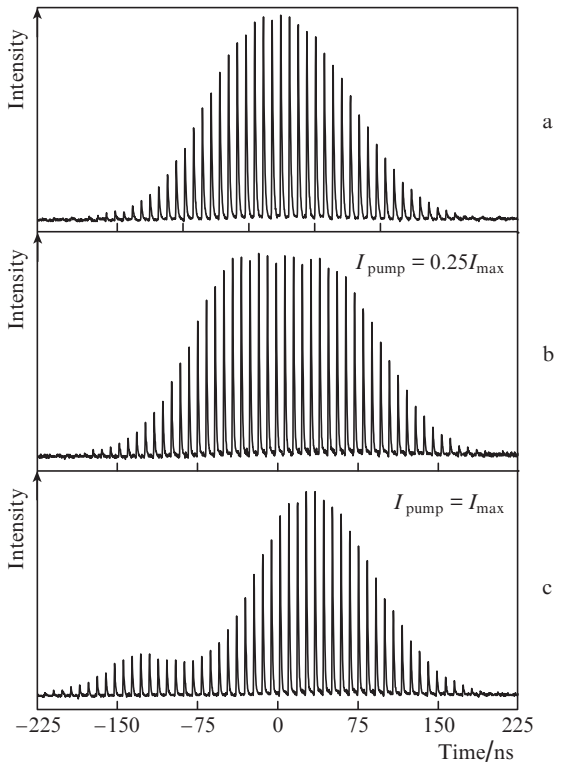

Figure 6. Oscillograms of pump pulse trains (λ_{exc} = 523.5 nm) at the (a) input and (b, c) output of $PbWO_4$ crystal ($\boldsymbol{E}\|C4$, $\boldsymbol{k}\perp C4$) at excitation intensities I = (b) $0.25I_{max}$ and (c) I_{max}.

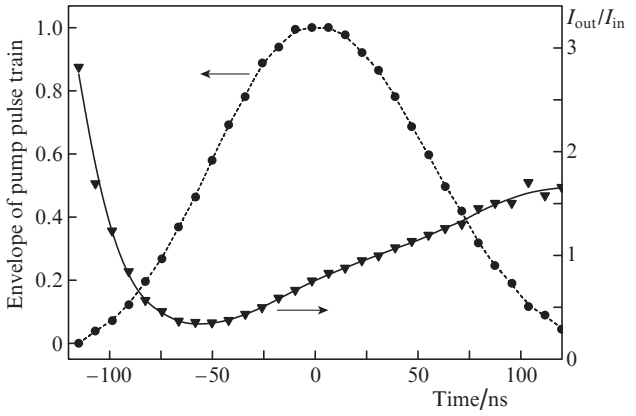

Figure 7. Time dependence of the transmittance (I_{out}/I_{in}) of $PbWO_4$ crystal excited by a picosecond-pulse train (λ_{exc} = 523.5 nm, $\boldsymbol{E}\|C4$, $\boldsymbol{k}\perp C4$).

4. Discussion

A model for analysing nonlinear parameters under interaction of high-power light with CdTe semiconductor structures was proposed in [11]. This model included the dependences of the refractive index on the light intensity, temperature, and concentration of free and bound carriers. The dependences of the nonlinear phase of radiation on the radiation intensity along the medium and the temperature dependence of the refractive index were analysed.

Without going into details of this analysis, we can note that the dependence of the nonlinear phase of radiation along the medium was determined, in particular, by the product of the nonlinear refractive index for bound electrons and the pump intensity, as well as by the thermo-optic and thermal-expansion coefficients. The dependence of the radiation intensity along the medium was determined by (i) the sum of the linear absorption coefficient and the product of the TPA coefficient and the pump intensity and (ii) the product of the absorption cross section and the concentration of photoinduced free carriers. The concentration of the latter depends on the TPA coefficient, recombination times of electrons and holes, and the diffusion coefficient (which determines the long-term relaxation processes). Thermal variations in the refractive index arise during the relaxation of TPA-excited carriers, nonradiative recombination, free-carrier absorption, and temperature gradient diffusion.

The difficulties of our analysis are related to the absence of data on most of the aforementioned coefficients for $PbWO_4$ crystals, except for our experimental data on the linear and two-photon absorption coefficients. Nevertheless, we tried to describe (on the time scale) the influence of a particular nonlinearity on the probe radiation kinetics.

Analysing the probe radiation oscillograms upon $PbWO_4$ crystal excitation by a train of high-power pulses and the formation of pulses in the spectrum of cw probe radiation, one can select three characteristic time ranges: from 0 to 100 ns (Fig. 3), from 100 ns to 100 μs, and from 100 μs to 1000 ms.

An analysis of the initial time range (0–100 ns) shows that the characteristic features related to the nonlinear TPA [14] are most pronounced when the spatial region of radiation detection is shifted [using diaphragm D (Fig. 1)] toward the wing of the profile of excitation pump and probe beams (Fig. 3). Specifically the exponential induced absorption front with a rise constant of 60 ns reflects the excitation generation kinetics.

The TPA-induced excitation of electron levels in the crystal conduction band and the instantaneous picosecond relaxation of electronic excitation to the metastable level lying in the crystal band gap are followed by a relatively slow (with characteristic times of ~10 μs) excitation migration between neighbouring WO_4^{2-} ions to trap (defect) levels [14].

The generation of a submillisecond positive pulse (Fig. 8) demonstrates the dynamics of the formation and decay (caused by thermal diffusion) of a thermal lens. Analyzing the oscillogram in Fig. 8, one can estimate the time of the thermal lens formation and decay. The lens formation time should

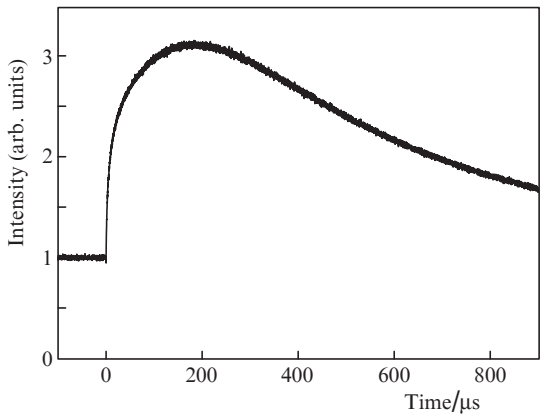

Figure 8. Oscillogram of thermal lens generation.

depend on the parameters of picosecond pump radiation (e.g., the pulse power and duration and the focusing conditions). The thermal lens formation with our pump radiation parameters is characterised by a sharp leading edge of the pulse in the time interval shorter than 10 μs, after which the rise of the pulse intensity slows down and stops after ~100 μs. The relatively slow thermal diffusion (for a time longer than 1 ms) makes the thermal lens decay.

The last stage, which describes the dynamics of nonlinear processes in the crystal, is completed by the migration of electronic excitation energy to trap levels with subsequent nonradiative and radiative relaxation from the excited states to the ground state with a characteristic time of ~100 ms (Fig. 2).

5. Conclusions

Thus, we investigated the dynamics of the nonlinear processes occurring upon interband excitation of a $PbWO_4$ crystal by a sequence of picosecond pulses and cw probe radiation in the range of times from several nanoseconds to several seconds. Time regions were revealed in which nonlinear TPA affects the enhancement and relaxation of the induced single-photon absorption in the nanosecond–second range. The processes related to the generation and migration of electronic excitations to traps were considered. It was shown that a thermal lens is induced in the paraxial region of picosecond excitation. The time intervals within which this lens is formed and decays as a result of thermal diffusion were determined. The relaxation electronic excitations from trap levels to the ground state were found to occur for times on the order of several hundreds of milliseconds. The transformation dynamics of the transmission spectrum was demonstrated for the degenerate picosecond two-photon excitation of crystal.

Acknowledgements. This work was supported by the Russian Foundation for Basic Research (Project No. 16-02-00338) and the Russian Scientific Foundation (Project No. 14-22-00248).

References

1. Prokhorov A.M. *Usp. Fiz. Nauk*, **85**, 599 (1965).
2. Prokhorov A.M. *Science*, **10**, 828 (1965).
3. Letokhov V.S. *Pis'ma Zh. Eksp. Teor. Fiz*., **7**, 284 (1968).
4. Gordon E.V., Moskvin Yu.L. *Zh. Eksp. Teor. Fiz*., **43**, 901 (1976).
5. Carman R.L. *Phys. Rev. A*, **12**, 1048 (1975).
6. Nikolaus B., Zhang D.Z., Toschek P.E. *Phys. Rev. Lett*., **47**, 171 (1981).
7. Gauthier D.J., Wu Q., Morin S.E., Mossberg T.W. *Phys. Rev. Lett*., **68**, 464 (1992).
8. Pfister O., Brown W.J., Stenner M.D., Gauthier D.J. *Phys. Rev. Lett*., **86**, 4512 (2001).
9. Rumi M., Perry J.W. *Adv. Opt. Photonics*, **2**, 451 (2010).
10. Gauthier D.J. *Prog. Opt*., **45**, 205 (2003).
11. Kaplan D.O., Kanter D.S., Kumar P. *Opt. Lett*., **21**, 1342 (1996).
12. Lukanin V.I., Chunaev D.S., Karasik A.Ya. *Pis'ma Zh. Eksp. Teor. Fiz*., **91**, 615 (2010).
13. Lukanin V.I., Chunaev D.S., Karasik A.Ya. *Zh. Eksp. Teor. Fiz*., **140**, 472 (2011).
14. Lukanin V.I., Karasik A.Ya. *Zh. Eksp. Teor. Fiz*., **144**, 235 (2013).
15. Lukanin V.I., Karasik A.Ya. *Opt. Commun*., **336**, 207 (2015).